EARTHQUAKE ENGINEERING AND STRUCTURAL DYNAMICS
Earthquake Engng Struct. Dyn. 2005; **34**:665–685
Published online 14 January 2005 in Wiley InterScience (www.interscience.wiley.com). DOI: 10.1002/eqe.449

Multi-objective framework for structural model identification

Yiannis Haralampidis, Costas Papadimitriou*,† and Maria Pavlidou

Department of Mechanical and Industrial Engineering, University of Thessaly, Pedion Areos, 38334 Volos, Greece

SUMMARY

Structural identification based on measured dynamic data is formulated in a multi-objective context that allows the simultaneous minimization of the various objectives related to the fit between measured and model predicted data. Thus, the need for using arbitrary weighting factors for weighting the relative importance of each objective is eliminated. For conflicting objectives there is no longer one solution but rather a whole set of acceptable compromise solutions, known as Pareto solutions, which are optimal in the sense that they cannot be improved in any objective without causing degradation in at least one other objective. The strength Pareto evolutionary algorithm is used to estimate the set of Pareto optimal structural models and the corresponding Pareto front. The multi-objective structural identification framework is presented for linear models and measured data consisting of modal frequencies and modeshapes. The applicability of the framework to non-linear model identification is also addressed. The framework is illustrated by identifying the Pareto optimal models for a scaled laboratory building structure using experimentally obtained modal data. A large variability in the Pareto optimal structural models is observed. It is demonstrated that the structural reliability predictions computed from the identified Pareto optimal models may vary considerably. The proposed methodology can be used to explore the variability in such predictions and provide updated structural safety assessments, taking into consideration all Pareto structural models that are consistent with the measured data. Copyright © 2005 John Wiley & Sons, Ltd.

KEY WORDS: structural identification; multi-objective optimization; Pareto set; reliability

1. INTRODUCTION

The problem of identifying the parameters of a structural model using dynamic data has received much attention over the years because of its importance in structural model updating, structural health monitoring and structural control. Comprehensive reviews of structural

*Correspondence to: Costas Papadimitriou, Department of Mechanical and Industrial Engineering, University of Thessaly, Pedion Areos, 38334 Volos, Greece.
†E-mail: costasp@uth.gr

Contract/grant sponsor: Greek Secretariat of Research and Technology
Contract/grant sponsor: Greek Earthquake Planning and Protection Organization (OASP)

Received 9 July 2003
Revised 12 March 2004
Accepted 15 October 2004

parameter identification methods can be found in References [1, 2]. The estimate of the parameter values involves uncertainties that are due to limitations of the mathematical models used to represent the behavior of the real structure, the presence of measurement error in the data, and insufficient excitation and response bandwidth. Structural identification and finite element model updating methodologies, for example, References [3–8], are often based on modal data since these data are readily obtained from well-established experimental structural dynamics techniques based on either forced [9, 10] or ambient vibration tests [11, 12]. The optimal structural models resulting from such methods can be used for response and reliability predictions, structural health monitoring and control.

Parameter identification problems based on measured data are often formulated as least-squares problems in which objective functions measuring the fit between measured and model predicted data are built up into a single objective using weighting factors. Standard optimization techniques are then used to find the optimal values of the parameters that minimize the overall measure of fit. The results of the optimization depend on the weighting factors assumed. The choice of the weighting factors depends on the model adequacy and the uncertainty in the available measured data, which are not known *a priori*.

In this work, the parameter identification problem is formulated in a multi-objective context that allows the simultaneous minimization of the multiple objectives, eliminating the need for using arbitrary weighting factors for weighting the relative importance of each objective. The set of admissible solutions are known in multi-objective optimization terminology as Pareto optimal solutions. The characteristics of the Pareto solutions are that they cannot be improved in any objective without causing degradation in one other objective. The set of Pareto solutions can be obtained using Evolutionary Algorithms [13] well-suited to solve multi-objective optimization problems [14, 15].

A multi-objective parameter identification framework for linear structures based on experimentally obtained modal data is presented. For this, the measured modal properties are grouped according to their characteristics (mode type, modal frequencies and modeshapes) and their significance on the objective of the identification. For each group, an objective function is introduced measuring the mismatch between the measured and the model predicted modal properties involved in the group. The Pareto optimal structural models are identified by minimizing these objectives simultaneously. The multi-objective problem is solved using a recently proposed Strength Pareto Evolutionary Algorithm [16] capable of identifying and representing the Pareto solutions with a few points uniformly distributed along the Pareto front [17]. The identified Pareto optimal structural models constitute acceptable compromise solutions trading-off the quality of fit in different groups of modal properties. The proposed methodology is illustrated by identifying the Pareto front and the corresponding set of Pareto optimal solutions for a model of a scaled laboratory structure using experimentally obtained modal data. These models are then used to predict the reliability of the structure to future stochastic loads modeled as stationary white noise processes. It is demonstrated that such predictions computed from the identified models along the Pareto optimal front may vary considerably.

The presentation in this work is organized as follows. In Section 2 the structural identification problem using measured modal data is formulated as a multi-objective optimization problem. The main concepts of evolutionary strategies and a recently proposed Strength Pareto Evolutionary Algorithm [16] for solving multi-objective minimization problems are outlined in Section 3. Applications on the multi-objective structural model identification methodology using measured data from a laboratory scaled building structure are presented in Section 4.

The variability in the predictions of structural reliability obtained by the identified Pareto optimal structural models is also addressed. For completeness, a discussion for extending the methodology to non-linear models based on measured response time histories, instead of modal properties, is presented in Section 5. The conclusions are summarized in Section 6.

2. MULTI-OBJECTIVE IDENTIFICATION BASED ON MODAL DATA

2.1. Formulation

Let $\hat{\omega}_r$ and $\hat{\boldsymbol{\phi}}_r \in R^{N_0}$ $(r=1,\ldots,M)$ be measured modal data from a structure, consisting of modal frequencies $\hat{\omega}_r$ and modeshape components $\hat{\boldsymbol{\phi}}_r$ at N_0 measured DOFs, where M is the number of observed modes. Consider a parameterized class of linear structural models (e.g. finite element models) used to model the dynamic behavior of the structure. Let $\boldsymbol{x}$ be the set of free model parameters to be identified using the measured modal data. These parameters are usually associated with geometrical, material, stiffness or mass properties and boundary conditions. The modal frequencies $\omega_r(\boldsymbol{x})$ and modeshapes $\boldsymbol{\phi}_r(\boldsymbol{x})$ predicted from the model class for a particular value of the parameter set $\boldsymbol{x}$ are obtained by solving the following eigenvalue problem

$$[K(\boldsymbol{x}) - \omega_r^2(\boldsymbol{x})M(\boldsymbol{x})]\boldsymbol{\phi}_r(\boldsymbol{x}) = \mathbf{0} \tag{1}$$

where $M(\boldsymbol{x})$ and $K(\boldsymbol{x})$ are the global model mass and stiffness matrices, respectively.

The objective in a modal-based structural identification methodology is to estimate the values of the parameter set $\boldsymbol{x}$ so that the modal data $\{\omega_r(\boldsymbol{x}),\ \boldsymbol{\phi}_r(\boldsymbol{x}),\ r=1,\ldots,M\}$ predicted by the linear class of models best matches, in some sense, the experimentally obtained modal data $\{\hat{\omega}_r,\ \hat{\boldsymbol{\phi}}_r,\ r=1,\ldots,M\}$. For this, the measured modal properties are grouped into n groups. Each group contains one or more modal properties. For the i-th group, a norm $J_i(\boldsymbol{x})$ is introduced to measure the mismatch between the measured modal properties involved in the group and the corresponding modal properties predicted from the model class for a particular value of the parameter set $\boldsymbol{x}$. The difference between the measured modal data and the model-based modal predictions is due to modeling and measurement errors always present in structural identification problems.

The problem of identifying the model parameter values that give the best fit in all groups of modal properties is formulated as a multi-objective optimization problem stated as follows. Find the values of the parameter set $\boldsymbol{x}$ that simultaneously minimizes the objectives

$$\boldsymbol{y} = \boldsymbol{J}(\boldsymbol{x}) = (J_1(\boldsymbol{x}),\ J_2(\boldsymbol{x}),\ \ldots\ J_n(\boldsymbol{x})) \tag{2}$$

where, using multi-objective terminology, $\boldsymbol{x} = (x_1, \ldots\ldots, x_m) \in X$ is the parameter vector, X is the parameter space, $\boldsymbol{y} = (y_1, \ldots\ldots, y_n) \in Y$ is the objective vector, and Y is the objective space. The optimization may be constrained due to restrictions imposed on the parameter set or to other constraints involved in the formulation. The feasible parameter space is usually confined in a hypercube by specifying lower and upper limits on each parameter. These limits depend on physical constraints, information about the physical characteristics of the system and modeling experience. Moreover, the search space can be confined to regions in the objective space for which the fit in the various modal properties are below a threshold value since solutions with high mismatch values in such properties are usually unacceptable. Constrained multi-objective

optimization problems are posed by considering the parameter space X to be confined in a region specified by the constraints.

For conflicting objectives $J_1(\boldsymbol{x}),\ldots,J_n(\boldsymbol{x})$, there is no single optimal solution, but rather a set of alternative solutions which are optimal in the sense that no other solutions in the search space are superior to them when all objectives are considered. Such alternative solutions, trading-off the fits in different modal group properties, are known in multi-objective optimization as Pareto optimal solutions.

Next, useful definitions related to the dominated and non-dominated vectors and Pareto solutions appearing in the multi-objective terminology [14, 15] are introduced. Specifically, a decision vector $\mathbf{a}\in X$ is said to dominate a decision vector $\mathbf{b}\in X$ (also written as $\mathbf{a}\prec\mathbf{b}$) if and only if

$$J_i(\mathbf{a})\leqslant J_i(\mathbf{b}) \quad \forall i\in\{1,\ldots,n\} \quad \text{and} \quad \exists j\in\{1,\ldots,n\}:\ J_j(\mathbf{a})<J_j(\mathbf{b}) \tag{3}$$

Additionally, we say $\mathbf{a}$ covers $\mathbf{b}$ ($\mathbf{a}\preceq\mathbf{b}$) if and only if $\mathbf{a}\prec\mathbf{b}$ or $\boldsymbol{J}(\mathbf{a})=\boldsymbol{J}(\mathbf{b})$. Based on the above relation, we can define non-dominated and Pareto optimal solutions as follows. A decision vector $\mathbf{a}\in X$ is said to be non-dominated regarding a set X if and only if there is no vector in X which dominates $\mathbf{a}$, that is, there is no vector $\mathbf{a}'\in X$ such that $\mathbf{a}'\prec\mathbf{a}$. All non-dominated vectors constitute admissible optimal solutions known in multi-objective optimization terminology as Pareto optimal solutions. The set of objective vectors $\boldsymbol{y}=\boldsymbol{J}(\mathbf{a})$ corresponding to the set of Pareto optimal solutions $\mathbf{a}$ is called Pareto optimal front. The characteristics of the Pareto solutions are that they cannot be improved in any objective without causing degradation in at least one other objective.

It should be noted that the parameter identification problem is traditionally solved by constructing a single objective from the multiple objectives, as follows

$$J(\boldsymbol{x})=\sum_{i=1}^{n} w_i J_i(\boldsymbol{x}) \tag{4}$$

using some weighting factors w_i, $i=1,\ldots,n$. The weights depend on the adequacy of the model class and the accuracy with which the measured modal data are obtained. More uncertain modal data should be given smaller weights. The results of the identification depend on the weights used. However, the choice of weights is arbitrary since the modeling error and the uncertainty in the measured data are usually not known *a priori*. The single objective is computationally attractive since conventional minimization algorithms can be applied to solve the problem.

Formulating the parameter identification problem as a multi-objective minimization problem, the need for using arbitrary weighting factors for weighting the relative importance of each objective is eliminated. An advantage of the multi-objective identification methodology is that all admissible solutions in the parameter space are obtained which constitute model trade-offs in fitting the different modal properties. These solutions are considered optimal in the sense that the fit in one modal group cannot be improved without deteriorating the fit in another modal group. The optimal points along the Pareto trade-off front provide detailed information about the quality of fit in the corresponding Pareto optimal models. The set of Pareto optimal solutions can be obtained using evolutionary algorithms well-suited to solve the multi-objective optimization problem. One such algorithm is the Strength Pareto Evolutionary Algorithm (SPEA) [16] described in Section 3.

2.2. Modal grouping and measures of fit

The grouping of the modal properties $\{\omega_r(\boldsymbol{x}),\ \boldsymbol{\phi}_r(\boldsymbol{x}),\ r=1,\ldots,M\}$ into n groups and the selection of the measures of fit $J_1(\boldsymbol{x}),\ldots,J_n(\boldsymbol{x})$ are usually based on user preference. The number and type of modal properties involved in the i-th group as well as the particular form of $J_i(\boldsymbol{x})$ may depend on the modal characteristics (mode type, modal frequencies and/or modeshapes), their expected uncertainties, and the significance of each modal property on the model identification. Among the various choices available, the following are considered for illustration purposes.

A group may be selected to contain the modal frequency and all modeshape components at the measured DOFs for a particular observed mode. In this case the number of groups equals the number of observed modes ($n=M$). The i-th measure of fit $J_i(\boldsymbol{x})$ accounts for the mismatch between the measured and the model predicted frequencies and modeshape components for the i-th measured mode. This grouping scheme is appropriate when the objective of the identification is to estimate all optimal models that trade-off the fit between different modes. Specifically, $J_i(\boldsymbol{x})$ can be given in the form

$$J_i(\boldsymbol{x})=\frac{\|\omega_i(\boldsymbol{x})-\hat{\omega}_i\|^2}{\|\hat{\omega}_i\|^2}+\frac{\|\boldsymbol{\phi}_i(\boldsymbol{x})-a_i\hat{\boldsymbol{\phi}}_i\|^2}{\|\hat{\boldsymbol{\phi}}_i\|^2},\quad i=1,\ldots,M \tag{5}$$

where $\|z\|^2=z^{\mathrm{T}}z$ is the usual Euclidian norm, and $a_i(\boldsymbol{x})=\boldsymbol{\phi}_i^{\mathrm{T}}(\boldsymbol{x})\hat{\boldsymbol{\phi}}_i/\|\hat{\boldsymbol{\phi}}_i\|^2$ is a normalization constant that accounts for the different scaling between the measured and the predicted modeshape for given $\boldsymbol{x}$. The set of objectives defined in Equation (5) is referred to as set A.

A second set of objectives, referred to as set B, can be defined by grouping the modal properties into two groups according to their type as follows. The first group contains all modal frequencies with the measure of fit selected to represent the mismatch between the measured and the model predicted frequencies for all modes, while the second group contains the modeshape components for all modes with the measure of fit selected to represent the mismatch between the measured and the model predicted modeshape components for all modes. Specifically, the two measures of fit can be given by

$$J_1(\boldsymbol{x})=\frac{1}{M}\sum_{r=1}^{M}\|\omega_r(\boldsymbol{x})-\hat{\omega}_r\|^2/\|\hat{\omega}_r\|^2 \tag{6}$$

and

$$J_2(\boldsymbol{x})=\frac{1}{M}\sum_{r=1}^{M}\|\boldsymbol{\phi}_r(\boldsymbol{x})-a_r\hat{\boldsymbol{\phi}}_r\|^2/\|\hat{\boldsymbol{\phi}}_r\|^2 \tag{7}$$

This selection allows one to estimate all Pareto optimal models that trade-off the overall fit in modal frequencies with the overall fit in the modeshapes.

3. EVOLUTIONARY ALGORITHM FOR MULTI-OBJECTIVE OPTIMIZATION

Evolutionary algorithms are well-suited for performing the multi-objective optimization. They process a set of promising solutions simultaneously and therefore are capable of capturing several points along the Pareto front. These algorithms are based on an arbitrarily initialized

population of search points in the parameter space, which by means of selection, mutation, and recombination evolves towards better and better regions in the search space. In this work, a recently proposed Strength Pareto Evolutionary Algorithm (SPEA) [16] based on evolution strategies is used for solving the multi-objective minimization problem. For completeness, the main concepts of evolution strategies for single-objective optimization are first introduced and then a brief outline of the SPEA method with its key features is presented.

3.1. Evolutionary strategies (ES)

Details on theoretical developments of evolution strategies (ES) can be found in Beyer [13]. The ES operates with populations of size (μ, λ) or $(\mu + \lambda)$, where μ is the size of the parent population and $\lambda \geqslant \mu \geqslant 1$ is the size of the offspring population. The members in a population are called individuals. Each individual is characterized by a vector of object variables $\boldsymbol{x} = (x_1, x_2, \ldots, x_m)^{\mathrm{T}}$, by an additional vector of strategy parameters $\boldsymbol{\sigma} = (\sigma_1, \sigma_2, \ldots, \sigma_m)^{\mathrm{T}}$, and by its fitness value $J(\boldsymbol{x})$, where $J(\boldsymbol{x})$ is the single objective function to be optimized. The population is evolved by the successive application of genetic operators on the population of individuals. These operators are selection, recombination and mutation. Each cycle of evolution is called generation. Each generation consists of a parent population of size μ. Using the genetic operators of recombination and mutation, λ offsprings are generated from the parent population, forming the population of descendants. Selection is then used to form the parent population in the next generation from the λ offsprings of the current population.

The genetic operations of recombination and mutation are discussed next. Recombination is applied not only to the object variables $\boldsymbol{x} = (x_1, x_2, \ldots, x_m)^{\mathrm{T}}$ but also the strategy parameters $\boldsymbol{\sigma} = (\sigma_1, \sigma_2, \ldots, \sigma_m)^{\mathrm{T}}$. Two kinds of recombination operators are used. The discrete recombination performed on the object variables and the intermediate recombination performed on the strategy parameters. In discrete recombination the offspring solution inherits its components from two parents chosen randomly with equal probability from the pool of parent population. Specifically, in generation g, the components x_i^g of the descendant $\boldsymbol{x}^g$ are generated from the components $x_{1,i}^g$ and $x_{2,i}^g$ of the two randomly selected parents $\boldsymbol{x}_1^g$ and $\boldsymbol{x}_2^g$ as follows:

$$x_i^g = x_{1,i}^g \text{ or } x_{2,i}^g \quad \text{with equal probability } 1/2 \tag{8}$$

Discrete recombination generates corners of the hypercube defined by the parents.

In intermediate recombination the offspring solution inherits components, which are a weighted average of the components from two parents $\boldsymbol{x}_1^g$ and $\boldsymbol{x}_2^g$ selected randomly from the pool of μ parents with equal probability $1/\mu$, according to the rule:

$$x_i^g = \alpha_i x_{1,i}^g + (1 - \alpha_i) x_{2,i}^g \tag{9}$$

where α_i is a scaling factor chosen uniformly at random over an interval $[0, 1]$. Intermediate recombination is capable of producing any point within a hypercube defined by the parents.

Mutations are typically implemented by adding to the parental recombination result $\boldsymbol{x}^g$ a Gaussian random vector $\boldsymbol{z}$ with independent components and distribution $N(0, \Sigma)$ as follows:

$$\tilde{\boldsymbol{x}}^g = \boldsymbol{x}^g + \boldsymbol{z} \tag{10}$$

The standard deviations (i.e. the square roots of the diagonal elements σ_i^2 of Σ) are called step sizes of the mutation and constitute the strategy parameters of the individual. A key feature

of ES is that they self-adapt these step sizes too. Specifically, the step size is modified by taking the product of itself with a log-normally distributed random number as follows:

$$\sigma_i \leftarrow \sigma_i \exp(z_0 + z_i) \tag{11}$$

where $z_0 = N(0,1)/\sqrt{2m}$ and $z_i = N(0,1)/\sqrt{2\sqrt{m}}$. The variable z_0 is computed once and is the same for all σ_i, while z_i is computed separately for each σ_i. As a result, general and specific scalings can be learned at the same time. The exponential function guarantees positive values for the mutation steps. In each generation every object variable and strategy parameter of an individual is mutated with the following order: (1) mutate strategy parameter, (2) mutate object variable.

3.2. The Strength Pareto Evolutionary Algorithm (SPEA)

The SPEA uses a number of features specific to multi-objective optimization algorithms for finding the multiple Pareto optimal solutions in parallel. Specifically, it stores in an external set the non-dominated solutions found in each generation. It uses the Pareto dominance concept in order to assign fitness values to individuals since the objective vector $\boldsymbol{y} = \boldsymbol{J}(\boldsymbol{x})$ defined in Equation (2) does not qualify as a scalar fitness function. The fitness of an individual is determined only from the solutions stored in the external non-dominated set. The solutions in the external set participate in the selection. It accomplishes fitness assignment and selection that guides the search towards the Pareto optima set. It maintains diversity in the population so that a well-distributed, wide-spread trade-off front is reached, preventing premature convergence to a part of the Pareto front. Finally, it performs clustering to reduce the number of non-dominated solutions.

The algorithm as proposed by Zitzler and Thiele [16] is the following:

Step 1: Generate an initial population P and create the empty external set P'.
Step 2: Copy non-dominated members of P to P'.
Step 3: Remove solutions within P' which are covered by any other member of P'.
Step 4: If the number of externally stored non-dominated solutions exceeds a given maximum N', prune P' by means of clustering.
Step 5: Calculate the fitness of each individual in P as well in P'.
Step 6: Select individuals from $P + P'$ (multiset union), until the mating pool is filled.
Step 7: Apply recombination and mutation to members of the mating pool in order to create a new population P.
Step 8: If the maximum number of generations is reached, then stop, else go to Step 2.

In Step 1 the initial population consists of μ parents chosen randomly from the feasible region in the parameter space.

In Step 5, all individuals in P and P' are assigned a scalar fitness value. This is accomplished in the following two-stage process. First, all members of the non-dominated set P' are ranked. Afterwards, the individuals in the population P are assigned their fitness value.
Stage 1: Each solution $i \in P'$ is assigned a real value $s_i \in [0,1)$ called strength s_i which is proportional to the number of population members $j \in P$ for which $i \preceq j$. Let n denote the number of individuals in P that are covered by i and assume N to be the size of P. Then s_i is defined as $s_i = \frac{n}{N+1}$. The fitness f_i of i is equal to its strength $f_i = s_i$.

Stage 2: The fitness of an individual $j \in P$ is calculated by summing the strengths of all external non-dominated solutions $i \in P'$ that cover j. Add one to this sum to guarantee that members of P' always have better fitness than members of P:

$$f_j = 1 + \sum_{i, i \preceq j} s_i \tag{12}$$

The stronger a non-dominated solution, the less fit are the covered individuals. The above ranking method gives a preference to individuals near the Pareto optimal front and distributes them along the trade-off surface.

In Step 6 the selection of individuals is done using the tournament selection procedure. Specifically, two individuals are selected randomly from $P + P'$ and the one with better fitness value is copied into the mating pool. This type of selection is elitism and ensures that good individuals do not get lost.

In Step 7 recombination and mutation is taking place. Discrete recombination is applied to the control variables and intermediate recombination to the step sizes according to the formulas (8) and (9). Mutation is done using the self-adaptive mutation method where the step size in each element in the mating pool is adapted according to (11).

In Step 4, the number of externally stored non-dominated solutions is limited to some number N'. This is necessary because otherwise P' would grow to infinity since there is always an infinite number of points along the Pareto-front. Moreover, one wants to be able to control the number of proposed possible solutions because, from a structural identification point of view, a few points along the front are often enough to provide a complete description of the wider variety of non-dominated structural models. The reason for introducing clustering is the distribution of solutions along the Pareto-front. In order to explore as much of the front as possible, the non-dominated members of P' should be equally distributed along the Pareto-front. Without clustering, the fitness assignment method would probably be biased towards a certain region of the search space, leading to an unbalanced distribution of the solutions. In this work the Single Linkage method [18] has been chosen for clustering.

4. APPLICATION

The multi-objective parameter identification framework is demonstrated using experimental modal data from a scaled two-story aluminum building model built and tested in the Structures Laboratory of the Hong Kong University of Science and Technology. The side and front views of the shear building model are given in Figure 1. The floors of the shear building are made of aluminum plates with dimensions $300 \times 300 \times 8$ mm. Each floor is supported by four columns and each column is made up of two identical aluminum bars with dimensions $38 \times 4.5 \times 274$ mm. The columns are connected to the floor and base plates through angles with the help of bolts and nuts. The structure was placed on a shake table and subjected to a base excitation. Acceleration response time histories at the two floors and the base along the weakest direction were obtained and the first two modes were identified using modal analysis software. The first two modal frequencies and modeshape components at the two floors are given in Table I. Details of the model, the experiments and the modal analysis performed to identify the modal frequencies and modeshapes can be found in Reference [19].

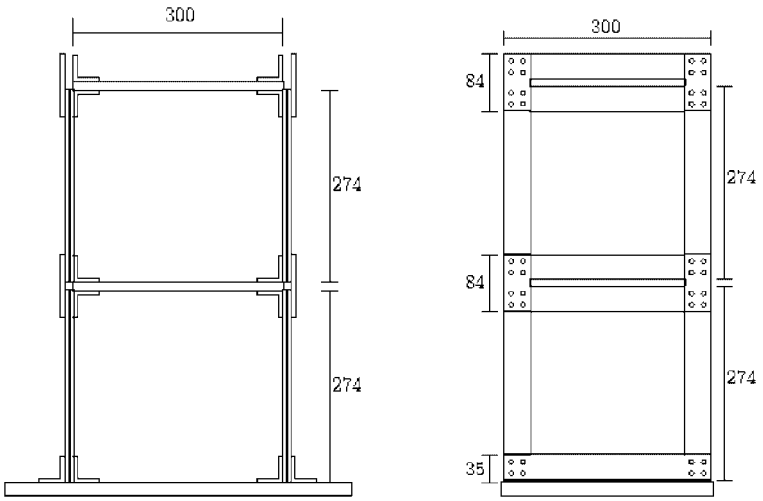

Figure 1. Side and front views of the shear building model (dimensions in mm).

Table I. Experimental modal frequencies and mode-shapes of the two-story aluminum building model.

		Mode 1	Mode 2
Modal frequencies (Hz)		17.2	50.4
Modeshapes	1st Floor	0.48	−1.23
	2nd Floor	1.00	1.00

4.1. Identification of a two-parameter model

The multi-objective parameter identification methodology is applied to identify the stiffness properties of the two floors. For this, the structure is modeled by a two-DOF linear lumped mass shear building model schematically shown in Figure 2. In the modeling, the masses are treated as deterministic, while the model parameters are chosen to be the two interstory stiffnesses of the two-story building. According to Reference [19], the model masses were estimated from the structural drawings to be $m_1 = 3.9562\,\text{kg}$ and $m_2 = 4.4482\,\text{kg}$. The *a priori* best estimate of the interstory stiffness calculated from the structural drawings is the same for both stories and equal to $k_0 = 2.3694 \times 10^5\,\text{N/m}$. The following parameterization of the two-DOF model shown in Figure 2 is used: $k_i = x_i k_0,\ i = 1, 2$. The purpose of the identification is to update the values of the stiffness parameters x_1 and x_2 using the measured modal data reported in Table I.

The set A of objectives defined in Equation (5) is first used to identify the Pareto optimal values of the parameter set $\boldsymbol{x} = (x_1, x_2)$. In order to identify and describe in detail the whole Pareto front, a high number $N' = 500$ of non-dominated solutions in the set P' is selected. The Pareto front, giving the Pareto solutions in the objective space, is shown in Figure 3 for

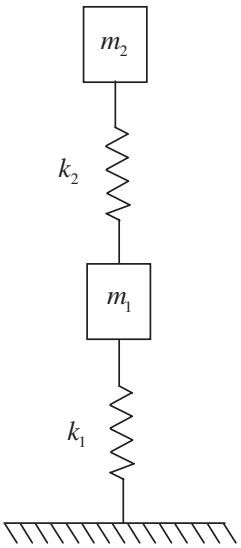

Figure 2. Two DOF lumped mass model.

$Ngen = 10$, 100, 1000 and 10000 number of generations. The corresponding Pareto optimal solutions in the parameter space are shown in Figure 4. The search for the Pareto optimal solutions was limited to the region defined by the inequality constraints $J_i(\boldsymbol{x}) \leqslant 0.05$ for $i = 1, 2$. Pareto solutions outside this range are considered unacceptable in structural identification due to the very high errors between measured and model predicted modal data involved in the measures of fit.

The large number of 10000 generations is used to approximate as close as possible the Pareto front and the Pareto optimal solutions. The results for 10, 100 and 1000 generations demonstrate the rate of convergence of the solutions provided by the SPEA algorithm. The results in Figure 3 suggest that as the number of generations increases the computed Pareto front converges closer to the Pareto front computed for 10000 generations. It should be noted that as the number of generations increases, the number of non-dominated solutions stored in the external set P' also increases. Figure 3 suggests that the allowable number of $N' = 500$ non-dominated solutions are obtained only when the number of generations is sufficiently high. For the small number of 10 and 100 generations, the number of non-dominated solutions in the set P' is smaller than $N' = 500$. In such cases clustering is not activated and as a result a non-uniform distribution of the non-dominated points along the Pareto front is obtained.

The results in Figure 4 suggest that the Pareto optimal solutions are concentrated in a narrow sub-region in the parameter space that extends along a one-dimensional manifold. The size of the sub-region perpendicular to the manifold decreases as the number of generations increases suggesting that the region approaches a one-dimensional manifold in the two-dimensional parameter space. These solutions correspond to interstory stiffness values which are significantly lower than the nominal stiffness values $x_1 = x_2 = 1$ estimated by structural drawings. This discrepancy is mainly due to modeling errors [19].

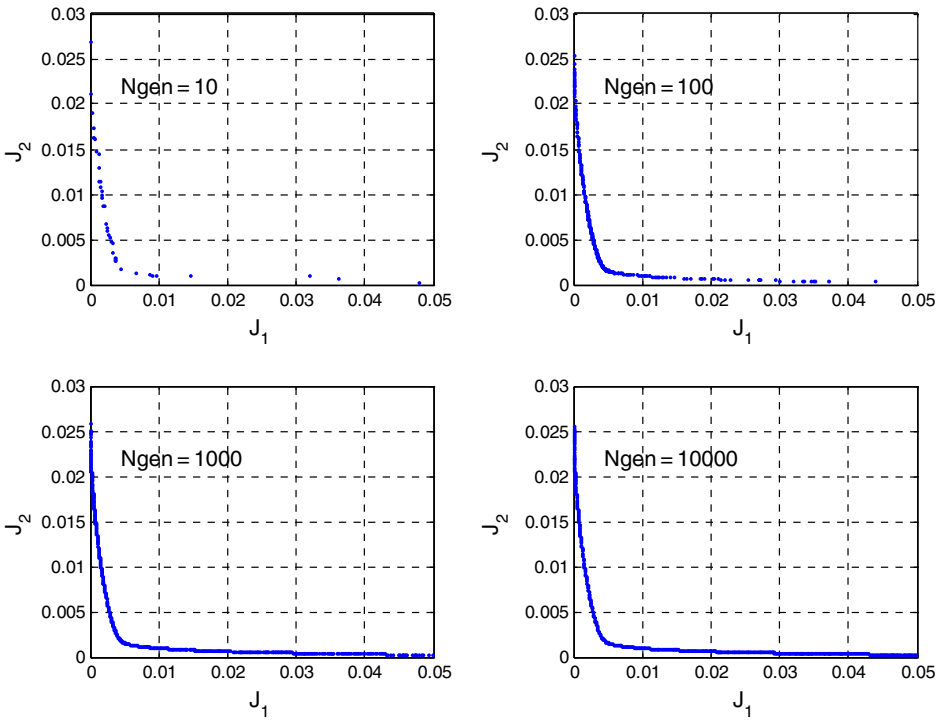

Figure 3. Pareto optimal solutions in objective space.

In order to evaluate the effectiveness of the proposed SPEA algorithm in adequately describing the Pareto front with a small number of points along it, the Pareto front and the corresponding Pareto solutions are also obtained for $N' = 20$ non-dominated solutions in the set P' using 200 generations. The results are shown in Figure 5 and are compared to the results obtained for the case of 1000 generations and $N' = 500$. The Pareto solutions for $N' = 20$ are numbered so that their correspondence in the objective and the parameter spaces becomes clear. It is seen that the $N' = 20$ points defining the Pareto front are uniformly distributed along the more detailed Pareto front represented by a high number of $N' = 500$ non-dominated solutions. Although the convergence in the parameter space has not been achieved with high accuracy, from the practical point of view the $N' = 20$ Pareto optimal solutions seem to give a very good representation of the Pareto front and the corresponding Pareto optimal models.

It is observed in Figure 5 that a wide variety of Pareto optimal solutions are obtained. These solutions are superior to all other solutions when both objectives are considered. Comparing the Pareto optimal solutions, there is no Pareto optimal solution that improves the fit in both measures simultaneously. Thus, all the Pareto solutions correspond to acceptable compromise structural models trading-off the fit in the modal properties of the two modes. The non-zero size Pareto front and the non-zero distance of the Pareto front from the origin are due to modeling and measurement errors.

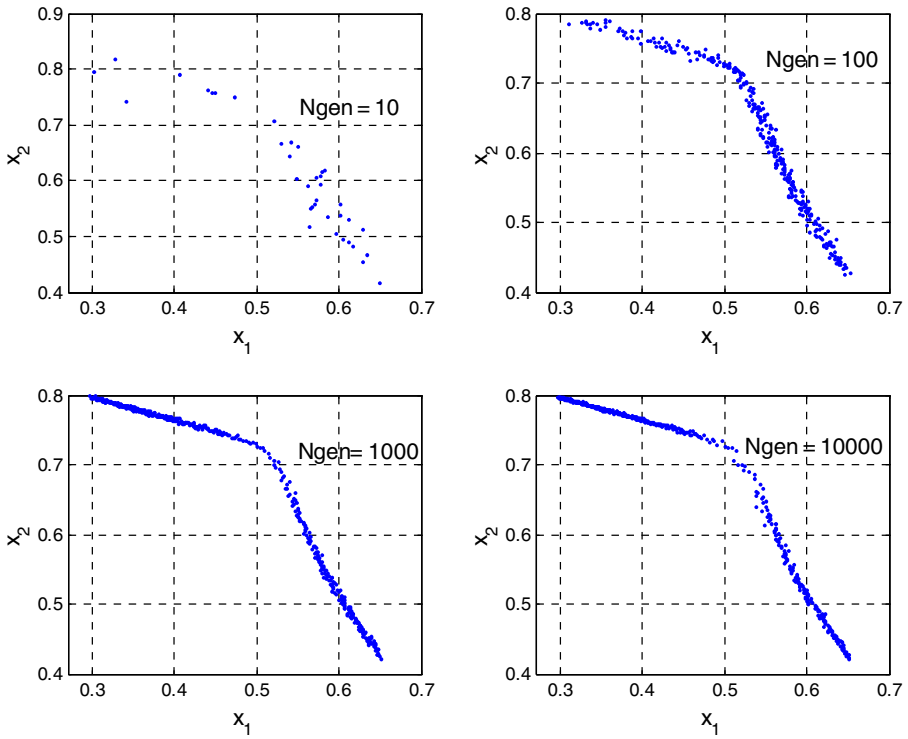

Figure 4. Pareto optimal solutions in parameter space.

Modeling errors, in particular, relate directly to the adequacy of the selected model class and are expected to be more significant than measurement errors. Therefore, the size of the Pareto front, the distance of the Pareto front from the origin, and the distance between the optimal structural models in the parameter space are mainly affected by the adequacy of the selected model class. For model classes that can exactly represent structural behavior and for error free measured data, the multi-objective identification methodology will in fact yield a zero-size Pareto front that consists of an isolated point located at the origin in the objective space. This is due to the fact that a solution $J_i(\boldsymbol{x}) = 0 \, \forall i = 1, \ldots, n \; (n = 2)$ exists which dominates all other solutions in the objective space. The corresponding optimal solutions in the parameter space may consist of either isolated points or an infinite number of points along a manifold, depending on whether the parameterized class of structural models is identifiable or unidentifiable [20–22], respectively, for the available measured data.

However, since it is unrealistic to expect that a model class can represent the underlying physical phenomena exactly, model errors will always be present and the proposed multi-objective structural identification will always yield a set of Pareto optimal solutions. In the present application, a simple parametric model class has been selected for updating in order to illustrate the proposed multi-objective identification framework. More adequate model classes such as detailed parametric finite element model classes will bring the Pareto front closer

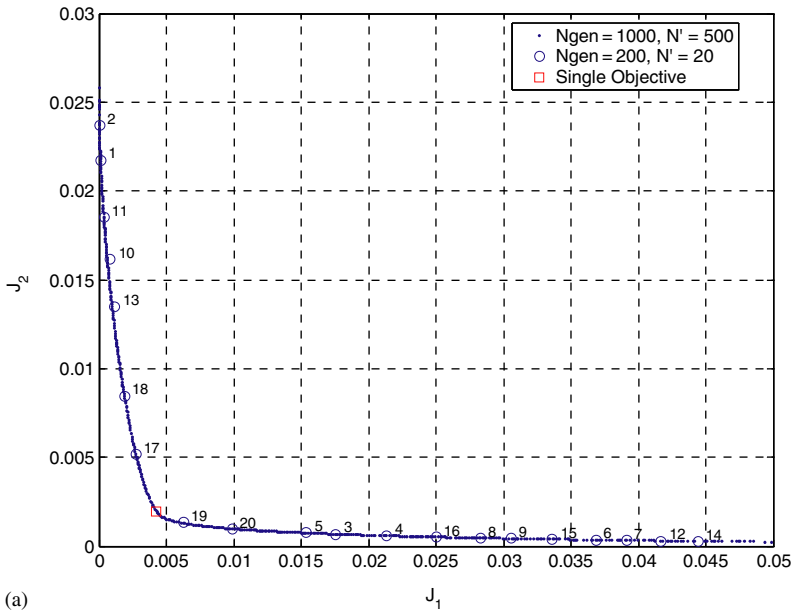

(a)

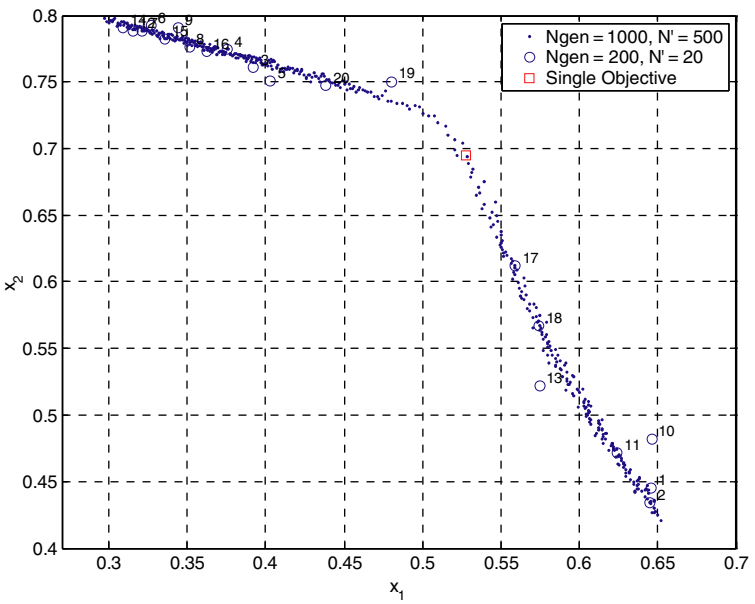

(b)

Figure 5. Pareto optimal solutions for set A in the region $J_i(\boldsymbol{x}) \leqslant 0.05$: (a) objective space; and (b) parameter space.

to the origin in the objective space, reducing the size of the Pareto front, and reducing the distance between the optimal models in the parameter space, thus improving the predictive accuracy of the model class.

Although a Pareto optimal structural model should always be a better compromise model than any model it dominates, not all Pareto optimal structural models may constitute acceptable compromise models. Information about the size of modeling and measurement errors is important for selecting a subset of optimal structural models along the Pareto front, eliminating unacceptable Pareto optimal solutions. For example, given that the fit in both measures is expected to be less than 0.01, one could disregard all Pareto solutions that fall outside the region of the objective space defined by $J_i(\boldsymbol{x}) \leqslant 0.01$ for $i = 1, 2$. Figure 6 shows the Pareto front and optimal solutions within the smaller region. There is still a wide variety of solutions with maximum distance between them in the parameter space equal to $d_{\max} = \max_{i,j \in P'} \|\boldsymbol{x}_i - \boldsymbol{x}_j\| = 0.252$.

There is a significant amount of information that can be extracted from the Pareto front and Pareto optimal solutions. For the sake of demonstration, let us assume that Pareto solutions are only acceptable if $J_i(\boldsymbol{x}) \leqslant J_0 \, \forall i = 1, \ldots, n$, i.e. the corresponding measures of fit are both below a pre-specified level J_0. The size of the Pareto front and the maximum distance $d_{\max}(J_0)$ between the acceptable solutions in the parameter space depends on the level J_0 selected in applications to reflect the size of modeling and measurement errors. The size of the region in the parameter space that provides alternative optimal solutions decreases as J_0 decreases. Moreover, there is a bound on $J_0 = 3.4 \times 10^{-3}$ below which the values of the two objectives cannot be reduced simultaneously. Such a bound is due to modeling error arising from the assumptions adopted in structural modeling, as well as measurement error present in the data. Specifically, the Pareto solution $\boldsymbol{x} = [0.546 \;\; 0.648]^{\mathrm{T}}$ maintains the fit for both measures to values close to $J_1(\boldsymbol{x}) = J_2(\boldsymbol{x}) = 3.4 \times 10^{-3}$ which is the minimal value that can be achieved for both measures simultaneously. It should be noted that the aforementioned solution differs by as much as $d = \|\boldsymbol{x} - \boldsymbol{x}_{\mathrm{so}}\| = 0.0508$ from the solution $\boldsymbol{x}_{\mathrm{so}} = [0.528 \;\; 0.695]^{\mathrm{T}}$ obtained by minimizing the single objective (4) with weighting factors $w_1 = w_2 = 0.5$. This difference is 20% of the maximum distance $d_{\max}$ between the Pareto optimal solutions in the parameter space.

Returning to the Pareto optimal solutions shown in Figure 5, it is observed that there is no other Pareto optimal solution that can improve the fit in both objectives to values less than 3.4×10^{-3}. However, there is a Pareto optimal model with $\boldsymbol{x} = [0.652 \;\; 0.420]^{\mathrm{T}}$ that improves the fit for the properties of the first mode to values as low as $J_1(\boldsymbol{x}) = 3.6 \times 10^{-7}$ at the expense of deteriorating the fit in the properties of the second mode to a value as high as $J_2(\boldsymbol{x}) = 0.0258$. This solution could be considered an acceptable one only if the objective of the identification is to construct a model that provides the best fit in the properties of the first mode, ignoring higher errors in the properties of the second mode. For example, this would be the case when there is information to support that measurement error is negligible in the modal properties involved in the first mode and that the parameterized structural model can accurately predict the properties of the first mode. Similarly, the Pareto optimal solution $\boldsymbol{x} = [0.297 \;\; 0.798]^{\mathrm{T}}$ shown in Figure 5 fits very well the modal properties of the second mode to values as low as $J_2(\boldsymbol{x}) = 3 \times 10^{-4}$ at the expense of deteriorating significantly the fit in the modal properties of the first mode to values as high as $J_1(\boldsymbol{x}) = 0.0499$. Similar interpretation can be given to this solution which can be accepted or rejected depending on the information available for the size of modeling and measurement errors.

Next, the Pareto optimal set is obtained for the two-parameter model using the set B of objectives defined in Equations (6) and (7). The first objective measures the overall mismatch of the modal frequencies, while the second one measures the overall mismatch of the

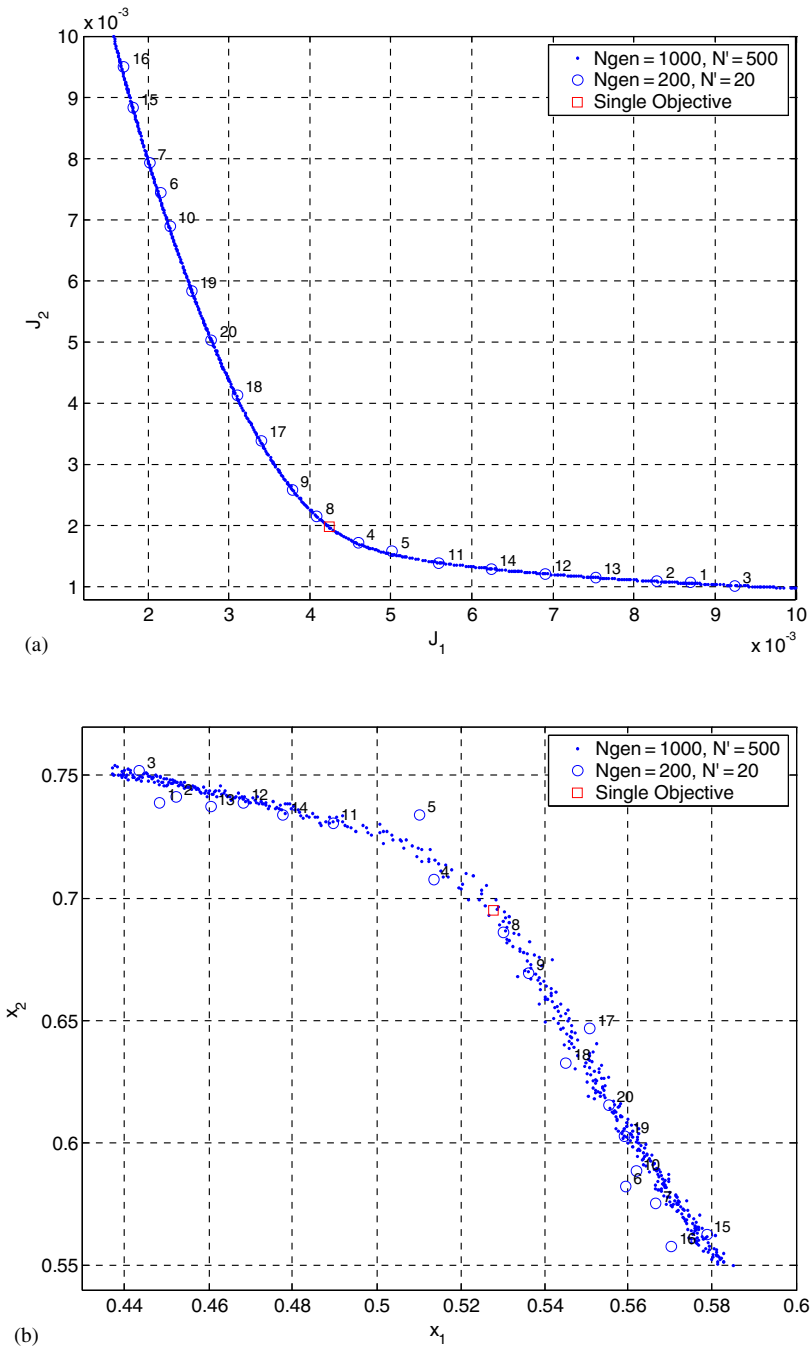

Figure 6. Pareto optimal solutions for set A in the region $J_i(\boldsymbol{x}) \leqslant 0.01$: (a) objective space; and (b) parameter space.

modeshape components. The Pareto front is shown in Figure 7(a) for 1000 generations and $N' = 500$ as well as for 200 generations and $N' = 20$. The corresponding Pareto solutions in the parameter space are shown in Figure 7(b). It is seen that the SPEA algorithm effectively distributes the solutions along the Pareto front so that the whole front is adequately described with a few points.

In contrast to the set A, the distance $d_{\max}(J_0)$ and the size of the Pareto front for the set B of objectives do not grow as J_0 increases. The Pareto optimal solutions shown in Figure 7(b) are concentrated in a relatively narrow sub-region in the parameter space. The values of the first objective, measuring the fit in the modal frequencies of both modes along the Pareto front, are in the range $J_1(\boldsymbol{x}) \in [1.5\times10^{-7},\ 0.002]$, while the values of the second objective, measuring the fit in modeshape components of both modes, are in the range $J_2(\boldsymbol{x}) \in [0.0026,\ 0.0032]$ which is a much narrower range than that for the modal frequencies. The best fit for the modeshape components cannot be less than $J_2(\boldsymbol{x}) = 2.6\times10^{-3}$. The fit in the modal frequencies can be substantially improved to as low as $J_1(\boldsymbol{x}) = 1.5\times10^{-7}$ at the expense of deteriorating by approximately 23% the fit in the modeshape components to the value $J_2(\boldsymbol{x}) = 3.20\times10^{-3}$. This could suggest that if the 23% difference in the fit in the modeshape components is not of concern in the identification, then among all Pareto optimal models, the model $\boldsymbol{x} = [0.511\ \ 0.718]^{\mathrm{T}}$ corresponding to $J_1(\boldsymbol{x}) = 1.5\times10^{-7}$ and $J_2(\boldsymbol{x}) = 3.20\times10^{-3}$ is most representative of the structure. The distance of this solution from the one obtained by minimizing the single objective (4) with weighting factors $w_1 = w_2 = 0.5$ is $d = 0.0286$ which is equal to 18% of the maximum distance $d_{\max} = \max_{i,j\in P'} \|\boldsymbol{x}_i - \boldsymbol{x}_j\| = 0.1571$ between the Pareto optimal solutions in the parameter space.

Finally, comparing the results in Figures 6 and 7 for the different sets A and B of objectives, it is clear that the Pareto optimal structural models also depend on the selection of modal properties involved in each modal group.

4.2. Structural reliability predictions using Pareto optimal models

The purpose of identification is to construct faithful structural models, within a selected model class, that can be used for making improved structural reliability predictions consistent with the measured data. The Pareto optimal set provides complete information about all optimal structural models consistent with the data that can be traded-off based on the accuracy they provide in the modal properties. The alternative models along the Pareto front provide different predictions of structural reliability which are all acceptable based on the measured data. Next the variability in the reliability predictions from all corresponding Pareto optimal models is explored.

The reliability of the structure given a model along the Pareto front can be computed using available probabilistic structural analysis tools. For simplicity, the reliability of the structure subjected to a base excitation that can be adequately modeled by white noise is considered. The system is considered to have failed under the stochastic base excitation if a response quantity $y(t;\boldsymbol{x})$ of the structure exceeds a threshold level b over a duration T. An estimate of the failure probability of the structure is obtained using well-known approximate random vibration results for linear structures. Specifically, for given model parameters $\boldsymbol{x}$, the probability of failure is approximated by [23]:

$$P(F|\boldsymbol{x}) = 1 - \exp[1 - 2\nu(\boldsymbol{x})T] \tag{13}$$

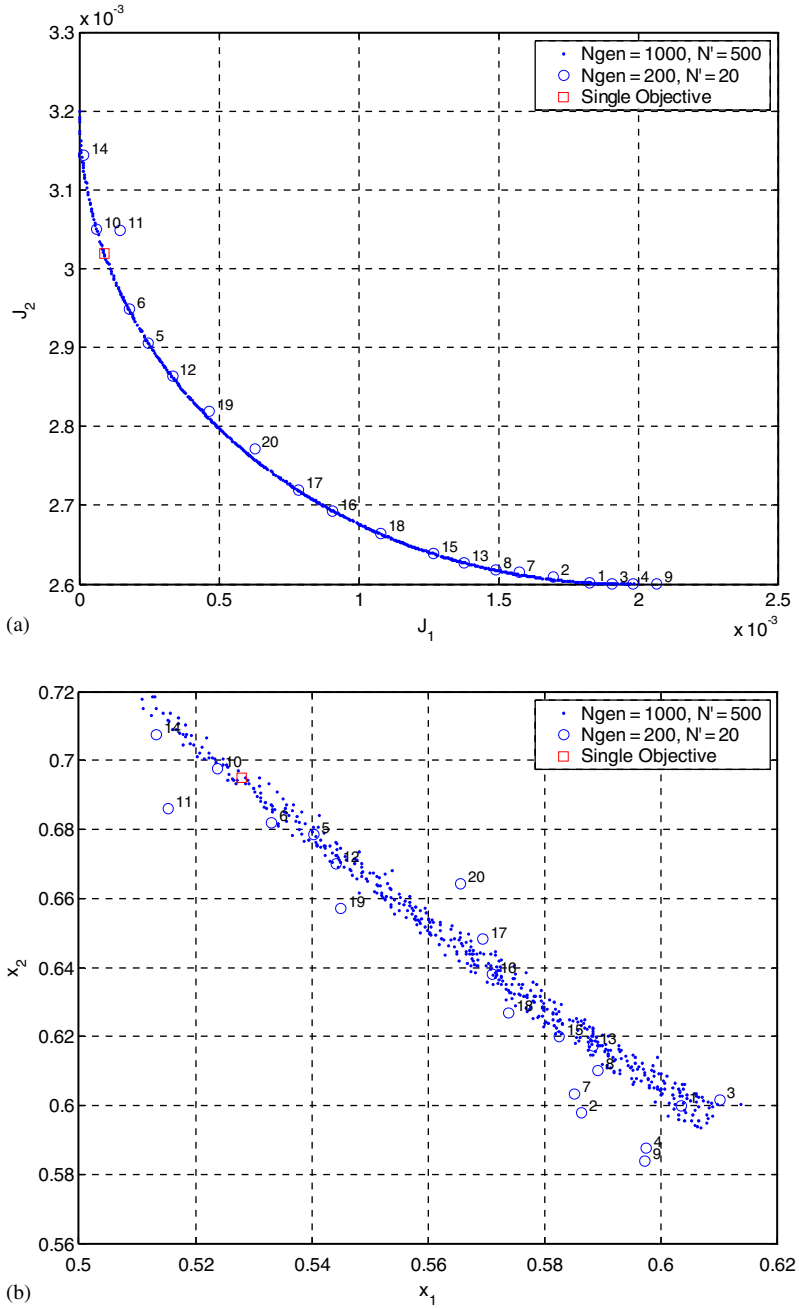

Figure 7. Pareto optimal solutions for set B: (a) objective space; and (b) parameter space.

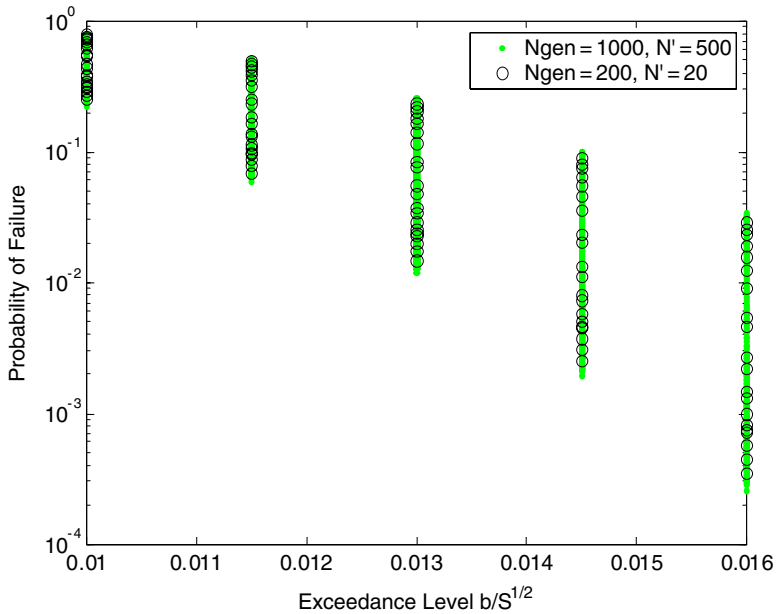

Figure 8. Reliability predictions based on all Pareto optimal structural models.

where $v(\boldsymbol{x})$ is the rate of outcrossing the level b, given by

$$v(\boldsymbol{x}) = \frac{1}{2\pi}\,\frac{\sigma_{\dot{y}}(\boldsymbol{x})}{\sigma_{y}(\boldsymbol{x})}\exp\left[-\frac{b^2}{2\sigma_{y}^2(\boldsymbol{x})}\right] \tag{14}$$

The quantities $\sigma_y(\boldsymbol{x})$ and $\sigma_{\dot{y}}(\boldsymbol{x})$ are the standard deviations of the response $y(t;\boldsymbol{x})$ and its derivative $\dot{y}(t;\boldsymbol{x})$, respectively. These standard deviations of the response are readily obtained for a linear system subjected to white excitation by using the Liapunov equation for the covariance matrix [23]. The reliability depends on the normalized threshold level $b/\sqrt{S}$, where S is the constant spectral density of the input white noise. More realistic descriptions of the base motion could readily be incorporated in the aforementioned formulation. It should be noted that accurate estimates of the probability of failure can also be obtained using efficient Monte Carlo techniques [24]. However, this is outside the scope of the present example.

In the numerical illustration, the structure is considered to have failed when the displacement response of the top floor exceeds a threshold level b. The probability of failure predicted by all Pareto optimal models for the set A of objectives is shown in Figure 8 for different normalized threshold levels $b/\sqrt{S}$. It can be seen that these predictions can vary considerably. Thus, the selection of a model among all Pareto optimal models has an impact on the reliability. Different models along the Pareto front result in different predictions. In general, the variability in the predictions depends on the adequacy of the model class selected for identification.

The results for the probability of failure in Figure 8, are computed and compared for a small number of $N' = 20$ non-dominated solutions and for a sufficiently large number of $N' = 500$ non-dominated solutions. It is evident that the failure probability bounds predicted by the

small number of $N' = 20$ non-dominated solutions match closely the more accurate failure probability bounds predicted by a very high number of $N' = 500$ non-dominated solutions. This means that from the prediction point of view, representation of the Pareto front by a small number of points, uniformly distributed along the front, is adequate.

5. EXTENSION TO NON-LINEAR STRUCTURES

The multi-objective parameter identification framework can readily be extended to identify the free parameter set $\boldsymbol{x}$ of a class of non-linear models of structures such as, for example, hysteretic models with various degrees of modeling sophistication (e.g. elastoplastic, bilinear, degrading, etc). In this case modal analysis is no longer applicable and the identification must be based on the experimentally obtained response time histories (e.g. accelerations, velocities, displacements), denoted by $\hat{y}_j(k\Delta t)$, where the index $j = \{1, \ldots, M\}$ refers to measurements at M DOFs, $k = 1, \ldots, N$ is the time index and Δt is the sampling period. For this, the measured response time histories are grouped into n groups with the i-th group g_i containing n_i response time histories such that $\sum_{i=1}^{n} n_i = M$. For the i-th group, a norm

$$J_i(\boldsymbol{x}) = \sum_{j \in g_i} \sum_{k=1}^{M} [y_j(k\Delta t; \boldsymbol{x}) - \hat{y}_j(k\Delta t)]^2 \tag{15}$$

is introduced to measure the mismatch between the measured response time histories involved in the group and the corresponding response time histories $y_j(k\Delta t; \boldsymbol{x})$ predicted from the non-linear model class for a particular value of the parameter set $\boldsymbol{x}$. The Pareto optimal solutions are then obtained by solving the multi-objective optimization problem stated in Equation (2). The estimation of $y_j(k\Delta t; \boldsymbol{x})$ involved in Equation (15) requires the solution of the non-linear set of differential equations governing the response of the non-linear structures.

The selection of the response time histories that are involved in a group is based on user preference and may depend on the number, location and type (e.g. displacement, velocity or acceleration) of measurements, as well as the information contained in the measurements about the free model parameters to be identified. For example, responses that contain significant information about the local non-linear properties of the structure could be included in the same group. In this way the fit of the responses in this group can be traded-off with the fit in another group containing information for another set of local or global properties of the structure.

Once the Pareto optimal non-linear models consistent with the measured data have been obtained, one could use these models to estimate the variability in the failure probability against various limit states which are indicative of damage, specified in terms of interstory drift for buildings, ultimate displacement, ductility demands, etc. For stochastic dynamic excitation, the estimation of structural reliability for each model along the Pareto front requires the integration into the formulation of efficient Monte Carlo techniques [25, 26].

6. CONCLUSIONS

A novel multi-objective framework for structural model identification based on modal data has been presented. Multiple objectives related to the fit between measured and model predicted

modal properties were simultaneously minimized, thus eliminating the need for arbitrarily weighting the relative importance of each objective in a single measure of fit. In contrast to the conventional weighted least-squares fit between measured and model predicted modal data, the proposed methodology provides multiple alternative optimal structural models consistent with the data in the sense that the fit each model provides in a group of modal properties cannot be improved without deteriorating the fit in at least one other group of modal properties. The multi-objective optimization problem can be solved using well-developed evolutionary algorithms. Specifically, the Strength Pareto Evolutionary Algorithm was effectively used for replacing the Pareto front by a relatively small number of representative optimal structural models, uniformly distributed along the Pareto front. These multiple Pareto optimal structural models are due to modeling and measurement errors. Information about the size of errors in the measured modal properties as well as information about the accuracy with which the selected class of structural models is expected to fit the modal frequencies and modeshape components used in the identification are important for selecting the acceptable optimal structural models along the Pareto front, eliminating unacceptable Pareto optimal solutions.

For the application considered, a wide variety of Pareto optimal structural models, uniformly distributed along the Pareto front, were obtained. The Pareto optimal solutions for the two-parameter model were concentrated in a narrow sub-region, extended along a certain direction in the parameter space. The variability of Pareto optimal models influences the predictions of structural reliability. Using the whole set of identified structural models, the failure probability of structures to future uncertain loads was predicted. It was demonstrated that such predictions from the Pareto optimal models may vary considerably. The proposed methodology can provide information about the failure probability bounds that are useful for making more informed structural safety assessments consistent with measured data.

Finally, the multi-objective identification framework is applicable to non-linear model identification based on response time histories.

ACKNOWLEDGEMENTS

This research was partially funded by the Greek Secretariat of Research and Technology within the EPAN program framework under grant DP15 and the Greek Earthquake Planning and Protection Organization. This support is gratefully acknowledged. The authors would like to thank Dr Paul H. F. Lam, Assistant Professor in the Department of Building and Construction, The City University of Hong Kong, for providing details on the experimental model and the measurements used in this work for illustrating the proposed multi-objective identification framework.

REFERENCES

1. Mottershead JE, Friswell MI. Model updating in structural dynamics: A survey. *Journal of Sound and Vibration* 1993; **167**(2):347–375.
2. Doebling SW, Farrar CR, Prime MB, Shevitz DW. Damage identification and health monitoring of structural and mechanical systems from changes in their vibration characteristics. A literature review. Los Alamos National Laboratory, Report No. LA-13070-MS, 1996.
3. Vanik MW, Beck JL, Au SK. Bayesian probabilistic approach to structural health monitoring. *Journal of Engineering Mechanics* (ASCE) 2000; **126**(7):738–745.
4. Bohle K, Fritzen CP. Results obtained by minimizing natural frequencies and MAC-value errors of a plate model. *Mechanical Systems and Signal Processing* 2003; **17**(1):55–64.
5. Hjelmstad KD, Shin S. Crack identification in a cantilever beam from modal response. *Journal of Sound and Vibration* 1996; **198**(5):527–545.

6. Friswell MI, Mottershead JE. *Finite Element Model Updating in Structural Dynamics*. Kluwer: Dordrecht, 1995.
7. Farhat C, Hemez PM. Updating finite element dynamics models using an element-by-element sensitivity methodology. *AIAA Journal* 1993; **31**(9):1702–1711.
8. Alvin KF. Finite element model update via Bayesian estimation and minimization of dynamic residuals. *AIAA Journal* 1997; **35**(5):879–886.
9. Ewins DJ. *Modal Testing—Theory*, *Practice and Applications*, (2nd edn.), Research Studies Press: U.K., 2000.
10. McConnnel KG. *Vibration Testing*: *Theory and Practice*. Wiley: New York, 1995.
11. Katafygiotis LS, Yuen KV. Bayesian spectral density approach for modal updating using ambient data. *Earthquake Engineering and Structural Dynamics* 2001; **30**:1103–1123.
12. Beck JL, May BS, Polidori DC. Determination of modal parameters from ambient vibration data for structural health monitoring. *First World Conference on Structural Control*, Los Angeles, 1994; 1395–1402.
13. Beyer HG. *The Theory of Evolution Strategies*. Springer: Berlin, 2001.
14. Fonseca CM, Fleming PJ. An overview of evolutionary algorithms in multiobjective optimization. *Evolutionary Computation* 1995; **3**(1):1–16.
15. Srinivas N, Deb K. Multiobjective optimization using nondominated sorting in genetic algorithms. *Evolutionary Computation* 1994; **2**(3):221–248.
16. Zitzler E, Thiele L. Multiobjective evolutionary algorithms: A comparative case study and the strength Pareto approach. *IEEE Transactions on Evolutionary Computation* 1999; **3**(4):257–271.
17. Mueller S, Walther J, Koumoutsakos P. Evolution strategies for film cooling optimization. *AIAA Journal* 2001; **39**(3):537–539.
18. Morse JN. Reducing the size of the nondominated set: Pruning by clustering. *Computers and Operations Research* 1980; **7**(1–2):55–66.
19. Lam HF. Structural Model Updating and Health Monitoring in the Presence of Modeling Uncertainties. *Ph.D. Thesis*, Department of Civil Engineering, Hong Kong University of Science and Technology, Hong Kong, 1998.
20. Beck JL, Katafygiotis LS. Updating models and their uncertainties. I: Bayesian statistical framework. *Journal of Engineering Mechanics* (ASCE) 1998; **124**(4):455–461.
21. Katafygiotis LS, Beck JL. Updating models and their uncertainties. II: Model identifiability. *Journal of Engineering Mechanics* (ASCE) 1998; **124**(4):463–467.
22. Katafygiotis LS, Lam HF. Tangential-projection algorithm for manifold representation in unidentifiable model updating problems. *Earthquake Engineering and Structural Dynamics* 2002; **31**:791–812.
23. Lutes LD, Sarkani S. *Stochastic Analysis of Structural and Mechanical Vibrations*. Prentice Hall: New Jersey, 1997.
24. Au SK, Beck JL. First excursion probability for linear systems by very efficient importance sampling. *Probabilistic Engineering Mechanics* 2001; **16**(3):193–207.
25. Pradlwalter HJ, Schueller GI. On advanced Monte Carlo simulation procedures in stochastic structural dynamics. *International Journal of Non-linear Mechanics* 1997; **32**(4):735–744.
26. Au SK, Beck JL. Estimation of small failure probabilities in high dimensions by subset simulation. *Probabilistic Engineering Mechanics* 2001; **16**(4):263–277.

